

Observing flare stars below 100 MHz with the LWA

Ivey Davis,[★] Greg Taylor[✉] and Jayce Dowell[✉]

Department of Physics and Astronomy, University of New Mexico, 210 Yale Blvd NE, Albuquerque, NM 81076, USA

Accepted 2020 April 6. Received 2020 March 23; in original form 2019 November 19

ABSTRACT

We observed the flare stars AD Leonis, Wolf 424, EQ Pegasi, EV Lacertae, and UV Ceti for nearly 135 h. These stars were observed between 63 and 83 MHz using the interferometry mode of the Long Wavelength Array. Given that emission from flare stars is typically circularly polarized, we used the condition that any significant detection present in Stokes I must also be present in Stokes V at the same time in order for us to consider it a possible flare. Following this, we made one marginal flare detection for the star EQ Pegasi. This flare had a flux density of 5.91 Jy in Stokes I and 5.13 Jy in Stokes V , corresponding to a brightness temperature $1.75 \times 10^{16} (r/r_*)^{-2}$ K.

Key words: stars: flare.

1 INTRODUCTION

Flares are not an uncommon event for magnetically active stars. For F- and G-type stars, there is a striking resemblance between these flares and solar flares, including the presence of both compact and two-ribbon flares, which conveniently allows for the implementation of a solar analogy for understanding the properties of these flares (Pallavicini, Tagliaferri & Stella 1990). Given the dependence of flaring on magnetic field dynamics, particularly on magnetic reconnection, it makes sense that M-dwarfs, which have been found to have magnetic field strengths of the order of kilo Gauss (Johns-Krull & Valenti 1996), would be particularly active.

One property of M-dwarfs that is of interest due to its probable role in the strength of the magnetic field is that they are entirely or near entirely convective (Reiners & Basri 2009). This characteristic means that stars with masses less than $0.35 M_\odot$ will lack the interface between the convective and radiative layer, which is related to the efficiency of magnetic field generation in solar-type stars (Charbonneau 2005). The interior dynamics may also affect the kind of dynamo effect involved in generating the magnetic field; while the Sun's field is heavily influenced by the α - ω dynamo, fully convective stars are more likely to have a field driven by convective turbulence (Durney, De Young & Roxburgh 1993; Yang et al. 2017). It has also been observed that the rotation period of the star is related to the magnetic field strength, so the rapid rotation of these stars likely also contributes to these magnetic fields with strengths thousands of times that of the solar magnetic field (Güdel 2002).

Radio emission of flare events has two main variants – coherent and incoherent (Benz & Güdel 2010). The cause of this emission is still being investigated; while some claim that electron cyclotron maser emission (ECM) is involved (Bastian & Bookbinder 1987;

Abdul-Aziz et al. 1995), the work of others indicate that ECM emission cannot be supported by their results (Abranin et al. 1998). Important factors that help discriminate the type of emission are the polarization and the duration of the flare. Emission is either strongly circularly polarized and short in duration or exhibits little to no polarization and is long lasting. The former suggests coherent emission like ECM or fundamental plasma emission and the latter is characteristic of gyrosynchrotron emission. In the circumstance of coherent emission, further details about the emission can be derived through the spectrum – since emission from a single maser is inherently narrowband, coherent, broadband emission implies either plasma emission or multiple maser sites being active.

The difficulty in understanding the emission process of flare stars, particularly M-dwarfs, is driven by the inconclusive results at frequencies below 1 GHz. Even within individual papers, results both support and oppose the solar analogy for stellar flares. There has been evidence of both negative frequency drifts – a feature of type II solar flares – as well as positive frequency drifts. Observations by Boiko et al. (2012) indicate frequent flaring at frequencies as low as 25 MHz, while Jackson, Kundu & Kassim (1990) and Lynch et al. (2017) find only marginal possible detections at 154 MHz. In order to better understand the origin of these discrepancies, we observed five nearby flare stars between 63 and 83 MHz.

2 METHODS

The five flare stars observed were AD Leonis (AD Leo), Wolf 424, EQ Pegasi (EQ Peg), EV Lacertae (EV Lac), and UV Ceti. Information on these stars is provided in Table 1. All of these stars are UV Ceti-type variables that have been detected at frequencies at least as low as ~ 1 GHz, are no farther than 10 pc away, and had transit elevations of at least 45° at the Long Wavelength Array (LWA) sites (a declination of -10°). The exception to this was UV Ceti, which had a transit elevation of about 37° .

* E-mail: idavis97@unm.edu

Table 1. Information on the flare star or flare star systems observed.

Star	Distance (pc)	Spectral type	RA (J2000)	Dec. (J2000)
AD Leo	4.9	M3.5eV	10 ^h 19 ^m 35 ^s .63	19°52'11".34
Wolf 424	4.3	dM6e/dM6e	12 ^h 33 ^m 15 ^s .22	09°01'19".42
EQ Peg	6.4	M3.5V/M4.5V	23 ^h 31 ^m 52 ^s .91	19°56'13".04
EV Lac	5.02	M3.5	22 ^h 46 ^m 48 ^s .51	44°19'54"
UV Ceti	2.68	M5.5V/M6V	01 ^h 39 ^m 05 ^s .65	-17°56'50"

Notes. The RA and Dec. provided here account for proper motion. The two values of spectral type given for Wolf 424, EQ Peg, and UV Ceti are due to the fact that they are binary systems. The coordinates and spectral type were provided by SIMBAD and the distances by Bastian (1990).

Table 2. Information on the flux and phase calibrator and check source used for the observations.

Star	Phase calibrator	Flux	Flux calibrator	Flux	Check source	Flux	Time on source (h)
AD Leo	3C 241	17.8	3C 295	125	3C 286	28.0	45.2
Wolf 424	4C 09.41	22.6	3C 295	125	4C 48.38	13.9	6.90
EQ Peg	4C 17.94	12.5	3C 48	67.6	3C 41	20.4	32.2
EV Lac	4C 46.47	11.2	3C 418	23.7	3C 415.2	21.6	29.9
UV Ceti	PKS 0139-16	17.1	3C 48	67.6	3C 41	20.4	20.7

Notes. The flux densities provided are in Jy, measured at 74 MHz. The locations and flux densities of the calibrators and check sources were provided by the NASA/IPAC Extragalactic Database (NED).

Observations of the flare stars were taken with the LWA, a dipole array with 256 elements at each of the sites. In order to distinguish the sources in the sky, the interferometry mode was used, employing the site near the Very Large Array (LWA1) and the site at the Sevilleta National Wildlife Refuge (LWA-SV), giving a \sim 70-km baseline. Such a separation aided not only in angular resolution, but also in mitigation of locale-specific radio frequency interference (RFI) during the correlation process. Two beams operated simultaneously at each site, allowing for simultaneous observing of calibrators and the source. One beam per site alternated between a flux and phase calibrator (calibration beam) and the other beam alternated between a check source – which served to confirm whether the beam was operating properly – and the flare star of interest (source beam). The phase calibrators chosen were within a few degrees of the respective star in order to account for ionospheric effects in the region of the star. Information on the phase and flux calibrators and the check sources are found in Table 2.

We spent a total of 134.88 h on source across the five stars, observing them at 68 and 78 MHz with a 9.8-MHz bandwidth for each of two frequency tunings (a total bandwidth of 19.6 MHz between 63.7 and 83.3 MHz). Following the observations, we used an LSL-based software correlator (Dowell et al. 2012) to correlate the data and provide an initial flag table. After correlation, we used AIPS in order to further flag and reduce the data. Signals in the calibration beam that appeared to be RFI were flagged and these flag tables were copied over to the source beam. There was further clean up in the source beam for signals that happened in single frequency channels and were short in time. Because flares are typically between a few seconds and several minutes, we looked at 1-, 10-, and 100-s integrations and averaged over the 20-MHz observing bandwidth to increase sensitivity for initial data reduction. Using this method, we were able to make a detection of the strong continuum source 4C 55.28, a 4.5-Jy source (see Fig. 1), placing a lower limit on our detection capabilities. An extra condition that was employed when deciding whether a flare was detected was the signal's presence in Stokes V due to the emission regularly being circularly polarized for brief flares (Lang & Willson 1986; Bastian & Bookbinder 1987; Osten et al. 2005; Lynch et al. 2017).

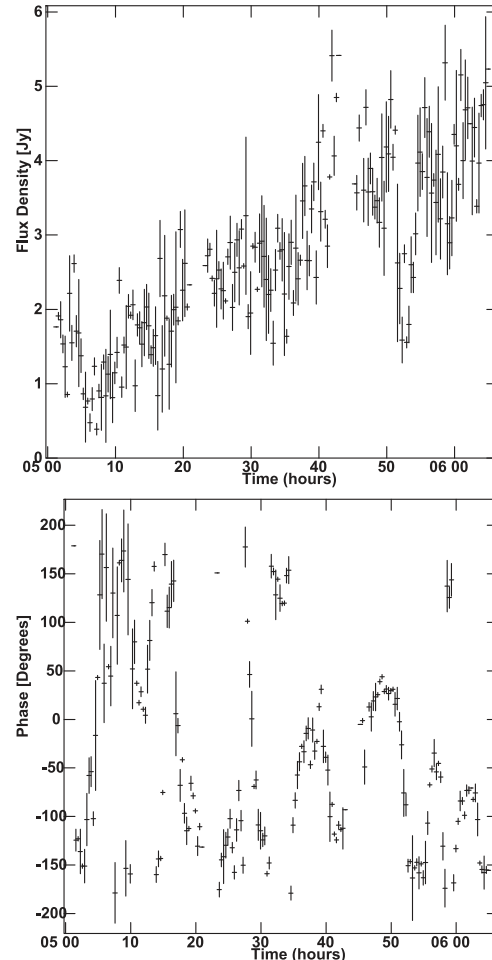


Figure 1. The 10-s integration of the source 4C 55.28 in Stokes I in flux versus time (top panel) and phase versus time (bottom panel) observed on 2018 May 28. The increasing flux density throughout the observation is a result of a similar trend in the calibration beam, but the distinct offset from 0 Jy of the signal makes us confident in the detection.

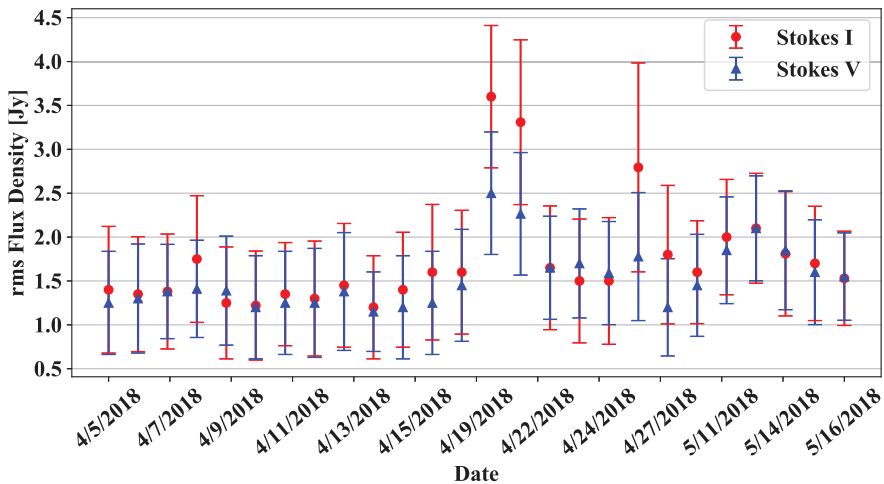


Figure 2. The rms and maximum values of 10-s integrations for each AD Leo observation; the marker is at the peak value and the rms is represented by the error bars.

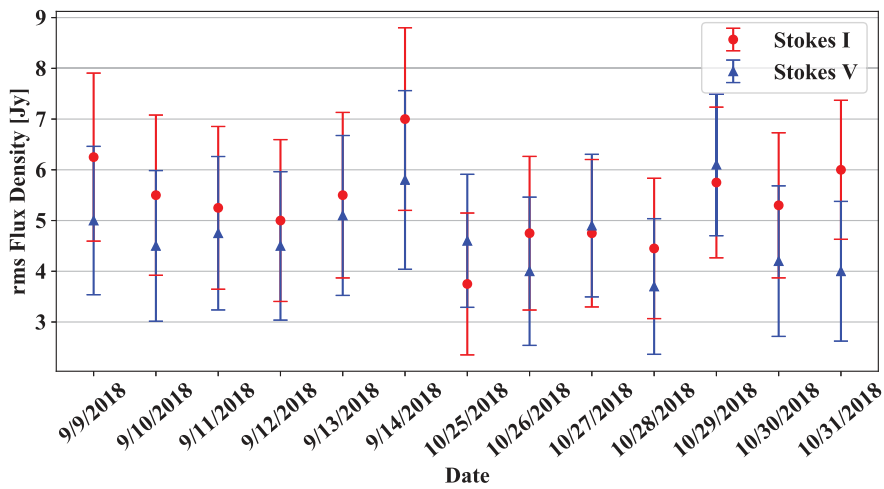


Figure 3. The rms and maximum values of 10-s integrations for each EV Lac observation.

3 RESULTS

3.1 AD Leo

AD Leo was observed for 45.2 h across 26 d from 2018 April 5 to May 17. From Fig. 2, the observations on April 21 and 22 appear to have significant detections in both Stokes I and V in the 10-s integrations; however, these peak values were not coincident, with their separations in time being as much as 4.5 min apart. These cases also showed no evidence of time evolution; rather than there being a rise and decay in the flux, these peak values corresponded to single instances, making it extremely unlikely they were true flare events.

3.2 Wolf 424

Wolf 424 is the flare star we have the least amount of information on as only 3 of the 14 scheduled observations were successful due to high ambient temperatures at one of the LWA sites, which prevented good operation. For these three observations, there is no evidence that a flare occurred. Because so little time was spent on this object

and the lack of detections, we cannot reasonably make any strong conclusions about the flaring properties or activity of Wolf 424.

3.3 EV Lac

EV Lac was observed for 29.9 h across 13 d in 2018 early September and late October. Although in Fig. 3, it would seem that the peak value in the observations of EV Lac were consistently significantly greater than the root mean square (rms), the flux density versus time plots for each observation show the flux density for both the star and the phase calibrator decreasing steadily throughout the observation. We attributed this trend to the proximity of EV Lac and 4C 46.47 to the Galactic plane during the observations, making it impossible to make conclusions about any possibly occurring flares at these low levels.

3.4 UV Ceti

UV Ceti was observed for 20.7 h across 9 d in 2019 late January and early March. In each observation, there was an apparent increase in

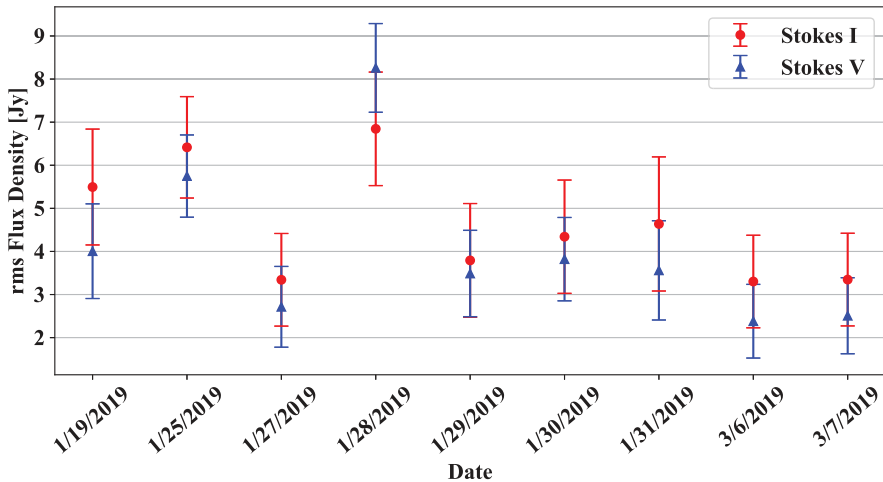


Figure 4. The rms and maximum values of 10-s integrations for each UV Ceti observation.

the flux density in both Stokes I and V in the last hour of the ~ 3 -h observation runs. This signal was consistently present in the 10-s integrations and often in the 100-s integrations as well. However, this signal was found to be due to a source passing through the fan beam that was centred on UV Ceti towards the end of the run. Because of the interference of the source, none of the peak values for these observations (see Fig. 4) can be attributed to flaring from the star and no other times during the observations showed evidence of flaring activity.

3.5 EQ Peg

EQ Peg was observed for a total of 32.2 h across 14 d from 2018 July 20 to November 13. There is strong evidence of a flare on July 20 at 11:27:10 UTC, shown in Fig. 5. While the flare reached about 5.91 Jy for Stokes V and 5.13 Jy in Stokes V for the 1-s integrations, it was only 2 Jy in Stokes I and 2.15 Jy in Stokes V during the 10-s integrations (Fig. 6) and was virtually absent during the 100-s integrations. This could be because of phases not adding coherently due to ionospheric effects.

4 DISCUSSION

Our best flare candidate was from EQ Peg on 2018 July 20. Although the signal for the flare was significantly diminished in the 10- and 100-s integrations, the flare lasted for ~ 30 s in the 1-s integrations. The absence of the flare during longer integrations, particularly in the 100-s integration, is likely the result of a rapidly varying phase due to a disturbed ionosphere. When averaged over the entire 19.6-MHz bandwidth, the Stokes I peak value of the flare was 5.91 Jy with an rms of 1.84 Jy for 1-s integrations. In Stokes V , the peak value was 5.13 Jy with an rms of 1.99 Jy. The fact that the flux density in Stokes V was so close to the value of the flare in Stokes I suggests that this signal was significantly circularly polarized, further supporting that this may have been a true flare event, making this the lowest frequency detection of EQ Peg to date.

When inspecting the calibration-corrected data prior to frequency averaging, no particularly strong channel was found in the cross-power spectrum in the time range of the flare, leading us to believe this was a broadband flare. Because the degree of our spectral analysis is so sensitivity-limited, this emission cannot be

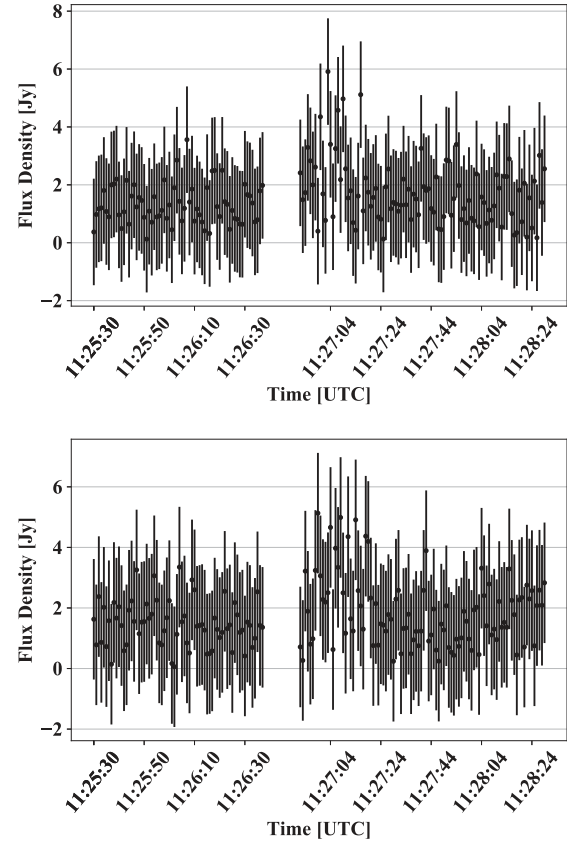


Figure 5. A slice from the 1-s integrations of EQ Peg on 2018 July 20, centred on the flare candidate at around UTC 11:27:05 in Stokes I (top panel) and Stokes V (bottom panel). The total height of the error bars is twice the rms of the observation.

differentiated between plasma emission or multiple ECM sites via observational results. When considering the magnetic and plasma environment of EQ Peg, we use magnetic field strengths of 480 G for EQ Peg A and 450 G for EQ Peg B (Morin et al. 2008) in the equation for cyclotron frequency in MHz (equation 1), where B is the magnetic field in Gauss, and gives cyclotron frequencies of 1.34

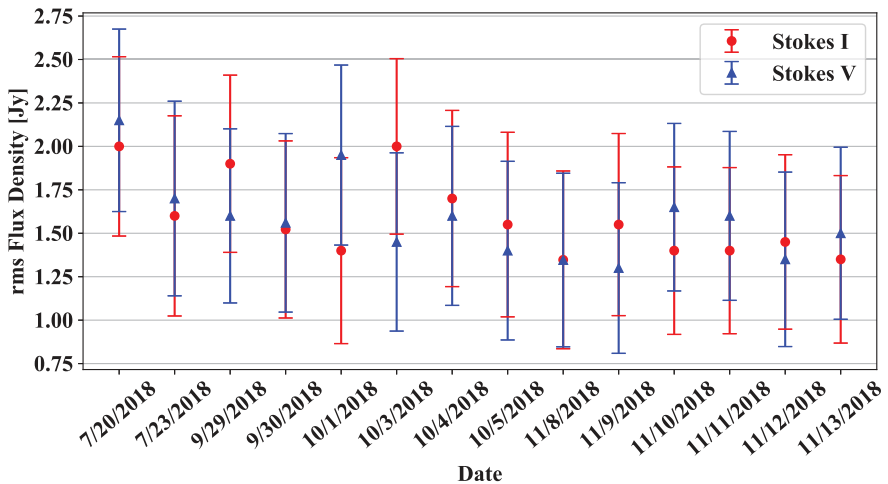


Figure 6. The rms and maximum values of 10-s integrations for each EQ Peg observation.

and 1.26 GHz for the A and B components, respectively:

$$v_{\text{cyc}} = \frac{eB}{2\pi m_e c} \approx 2.8B, \quad (1)$$

To calculate the plasma frequency, we use equation (2), where m is the effective mass of the electron, q is the electric charge, and n is the electron number density. Using 3×10^{11} and $4 \times 10^{10} \text{ cm}^{-3}$ as the upper and lower limits on the number density of EQ Peg's corona (Liefke et al. 2008) gives plasma frequencies of 4.92 and 1.80 GHz for the upper and lower plasma density estimates, respectively. This puts the fraction v_{cyc}/v_p between 0.26 and 0.75. For fundamental ECM emission to escape, $v_{\text{cyc}}/v_p \gtrsim 1$, although harmonic emission is possible for $2v_{\text{cyc}}/v_p > 1$ and thus is a possibility. Because either emission process should be possible even for the globally averaged magnetic field strength and number density, as well as the fact that local conditions may exist in the field and plasma not accounted for in the average values that would make even fundamental ECM possible, we cannot rule out ECM or plasma emission as being responsible for this flare in this way:

$$v_p = \frac{1}{2\pi} \sqrt{\frac{4\pi n q^2}{m}} \approx 9000\sqrt{n}. \quad (2)$$

Using equation (3), where T_B is the brightness temperature, S_ν is the flux density, D is the distance to the source, and r_s is the radius of the emission source, we find $T_B = 1.75 \times 10^{16} (r/r_*)^{-2}$ K assuming a stellar radius $r_* = 0.23 R_\odot$ (White, Jackson & Kundu 1989), a temperature achievable for both ECM and fundamental plasma emission. Although the duration of this flare (~ 30 s) is reminiscent of the duration of the broadband, plasma emission related type III solar bursts, the polarization of type III bursts is little to none at low frequencies (Reid & Ratcliffe 2014). The likely ECM-driven type IV bursts are also broadband and highly circularly polarized. However, this kind of burst is often longer in duration (> 10 min; Liu et al. 2018), although this duration difference could possibly be accounted for by a difference in beaming geometry between EQ Peg and the Sun should ECM be the responsible process. It is also possible that the flare lasted longer, but we were only able to detect it during the time it was brightest. Without a good solar analogy with which to compare this flare event to, we are still unable to determine the emission process beyond it likely being fundamental

plasma or ECM emission:

$$T_B = \frac{S_\nu}{2k} \frac{c^2}{\nu^2} \frac{D^2}{\pi r_s^2}. \quad (3)$$

The possible processes' dependence on the environment of the star, and this environment's variability, could explain why there is such variability in what frequencies EQ Peg – as well as other flare stars bright in the radio – can be seen at as well as in what processes are predicted to be responsible. EQ Peg has been successfully detected at frequencies as high as 1.4 GHz (Kundu et al. 1988; Jackson, Kundu & White 1989) and as low as 320 MHz (Crosley & Osten 2018); however, observations conducted by Arecibo at 430 MHz show no evidence of flaring activity (Spangler & Shawhan 1976). Similar results are found for AD Leo; coordinated observations of AD Leo with the Clark Lake Radio Observatory and VLA had only two brief detections at 110.6 MHz but found it was consistently flaring in the time between those two detections at 1.4 GHz (Jackson et al. (White, Kundu & Jackson 1986; Kundu et al. 1988; Jackson et al. 1990). However, using the UTR-2 array, Boiko et al. (2012) made as many as 30 detections on a single day of observation with the flux density of the flares ranging between 4 and 300 Jy at frequencies between 16.5 and 33 MHz. Although instrumental limitations or error could very well account for this, it is also not unlikely that the variability of the environment of young stars with strong magnetic fields would drastically affect the emission frequency for processes that so heavily depend on the plasma density.

5 SUMMARY

Many stars have been shown to exhibit flaring properties similar to those presented by the Sun across many parts of the electromagnetic spectrum. However, results below 1 GHz have been largely inconclusive with observations showing a huge variety in the frequency of the events, the wavelength at which they occur, the drift rate, flux density, and size of the area that the signal must be originating from. The goal of the observations presented here was to provide further restrictions for these properties for low frequencies. Although only one detection was made across the 130 h spent on five flare stars, the properties of the flare from EQ Peg are consistent with characteristics of either ECM or fundamental plasma emission. This flare was broadband as well as had a brief duration –

suggesting a similar emission process as type III bursts solar flares – and was strongly circularly polarized like type IV bursts. Without the possibility of better spectral analysis, a better understanding of the plasma density and magnetic field topologies, or an all-encompassing solar burst analogy, we cannot adequately discern which of the two processes was responsible. Given the dependence of these processes on the coronal properties of the star, and that these properties are subject to significant variability for stars with strong, variable magnetic fields, it seems likely that our low duty cycle was heavily affected by the nature of the emission process.

Although the nature of the possible emission processes was likely a significant contributor to the difficulty in detecting flares, the sensitivity of the two-element LWA may very well be an issue, especially in the case of AD Leo, which received the most observation time and for which we still made no detections, despite having been observed at similar frequencies by others. Some obstacles encountered for observations of the other flare stars were the LWA shutting down to avoid overheating and interference from other sources in the fan beam.

Ideally, coordinated observations at a variety of frequencies should be conducted for objects that did not experience confusion from other sources passing through the fan beam (AD Leo, Wolf 424, and EQ Peg) in order to better discern whether the low duty cycle is due to the sensitivity or the frequency range – and, consequently, the emission process. For objects that experienced significant confusion (EV Lac and UV Ceti), we need to choose observation times that better exclude the interfering sources without sacrificing too much of the time which the source spends close to its transit height. Despite only confidently detecting one flare, this flare provided the lowest frequency detection of EQ Peg to date and confirms the LWA as a viable instrument in stellar research at frequencies below 100 MHz. The sensitivity of the observations can be improved with the implementation of the LWA Swarm concept (Dowell & Taylor 2018), which would allow for imaging the fields and consequently self-calibration to remove ionospheric effects and thus allow longer integrations.

ACKNOWLEDGEMENTS

Construction of the LWA has been supported by the Office of Naval Research under Contract N00014-07-C-0147 and the AFOSR. Support for operations and continuing development of the LWA1

is provided by the Air Force Research Laboratory and the National Science Foundation under grants AST-1835400 and AGS1708855. We would also like to thank Stephen White and the reviewer for their input.

REFERENCES

Abdul-Aziz H. et al., 1995, *A&AS*, 114, 509
 Abranin E. P. et al., 1998, *Astron. Astrophys. Trans.*, 17, 221
 Bastian T. S., 1990, *Sol. Phys.*, 130, 265
 Bastian T. S., Bookbinder J. A., 1987, *Nature*, 326, 678
 Benz A. O., Güdel M., 2010, *ARA&A*, 48, 241
 Boiko A. I., Konovalenko A. A., Koliadin V. L., Melnik V. N., 2012, *Adv. Astron. Space Phys.*, 2, 121
 Charbonneau P., 2005, *Living Rev. Sol. Phys.*, 2, 2
 Crosley M. K., Osten R. A., 2018, *ApJ*, 856, 39
 Dowell J., Taylor G. B., 2018, *J. Astron. Instrum.*, 7, 1850006
 Dowell J., Wood D., Stovall K., Ray P. S., Clarke T., Taylor G., 2012, *J. Astron. Instrum.*, 1, 1250006
 Durney B. R., De Young D. S., Roxburgh I. W., 1993, *Sol. Phys.*, 145, 207
 Güdel M., 2002, *ARA&A*, 40, 217
 Jackson P. D., Kundu M. R., White S. M., 1989, *A&A*, 210, 284
 Jackson P. D., Kundu M. R., Kassim N., 1990, *Sol. Phys.*, 130, 391
 Johns-Krull C. M., Valenti J. A., 1996, *ApJ*, 459, L95
 Kundu M. R., Pallavicini R., White S. M., Jackson P. D., 1988, *A&A*, 195, 159
 Lang K. R., Willson R. F., 1986, *ApJ*, 305, 363
 Liefke C., Ness J. U., Schmitt J. H. M. M., Maggio A., 2008, *A&A*, 491, 859
 Liu H. et al., 2018, *Sol. Phys.*, 293, 58
 Lynch C. R., Lenc E., Kaplan D. L., Murphy T., Anderson G. E., 2017, *ApJ*, 836, L30
 Morin J. et al., 2008, *MNRAS*, 390, 567
 Osten R. A., Hawley S. L., Allred J. C., Johns-Krull C. M., Roark C., 2005, *ApJ*, 621, 398
 Pallavicini R., Tagliaferri G., Stella L., 1990, *A&A*, 228, 403
 Reid H. A. S., Ratcliffe H., 2014, *Res. Astron. Astrophys.*, 14, 773
 Reiners A., Basri G., 2009, *A&A*, 496, 787
 Spangler S. R., Shawhan S. D., 1976, *ApJ*, 205, 472
 White S. M., Kundu M. R., Jackson P. D., 1986, *ApJ*, 311, 814
 White S. M., Jackson P. D., Kundu M. R., 1989, *ApJS*, 71, 895
 Yang H. et al., 2017, *ApJ*, 849, 36

This paper has been typeset from a \TeX / \LaTeX file prepared by the author.